Nano Energy (2014) 4, 65–72

Available online at www.sciencedirect.com

ScienceDirect

journal homepage: www.elsevier.com/locate/nanoenergy

RAPID COMMUNICATION

Aligned carbon nanotube/sulfur composite cathodes with high sulfur content for lithium-sulfur batteries

Xin-Bing Cheng, Jia-Qi Huang, Qiang Zhang*, Hong-Jie Peng, Meng-Qiang Zhao, Fei Wei

Beijing Key Laboratory of Green Chemical Reaction Engineering and Technology, Department of Chemical Engineering, Tsinghua University, Beijing 100084, China

Received 18 October 2013; accepted 21 December 2013
Available online 30 December 2013

KEYWORDS
Lithium sulfur battery;
Aligned carbon nanotube;
Energy storage;
Cathode;
Composite

Abstract
The use of conductive carbon scaffolds is efficient and effective to obtain advanced composite cathodes for lithium-sulfur batteries. However, the loading amount of mostly less than 70 wt% induces a limited energy density and the typical fabrication route involving high-temperature and elaborate process also limits the manufacturability of sulfur cathode, both of which hinder the practical application of lithium-sulfur batteries. Herein, a scalable, room-temperature, and one-step method is employed for carbon nanotube (CNT)/sulfur composite cathode, in which aligned CNTs served as interconnected conductive scaffolds to accommodate sulfur. When the loading amount of sulfur increased from 50 to 90 wt%, the tap density of CNT/sulfur increased from 0.4 to 1.98 g cm^{-3}, and the mass/areal/volumetric capacities of the whole electrodes (CNT/sulfur composites and binders) was improved from 500.3 mAh g^{-1}/0.298 mAh cm^{-2}/200.1 mAh cm^{-3} to 563.7 mAh g^{-1}/0.893 mAh cm^{-2}/1116.0 mAh cm^{-3}, respectively. The rise of sulfur content in the composite cathode renders a dramatic increase of the energy density of lithium-sulfur cells. The ultra-high loading amount of sulfur is attributed to the open, ordered, straight pore structure of aligned CNT scaffolds for the uniform distribution of fine sulfur particles. The robust sp^2 carbon frameworks served as rapid pathways for electron transfer, and the large aspect ratio, good alignment, ordered packing of individual CNT in small bundles offer a low conductive percolation threshold. Consequently, the sulfur with a high loading content was efficiently utilized for a lithium-sulfur cell with a much improved energy density.

Introduction

Lithium ion batteries are one of the most important power sources for portable and moderately powered electronic

*Corresponding author.
E-mail address: zhang-qiang@mails.tsinghua.edu.cn (Q. Zhang).

2211-2855/$ - see front matter © 2013 Elsevier Ltd. All rights reserved.
http://dx.doi.org/10.1016/j.nanoen.2013.12.013

applications. With tremendous efforts from scientific and engineering communities, the energy density both in mass and volume of lithium ion batteries are nearly approaching the theoretical limits [1,2]. However, it still cannot fulfill the demand of environment-friendly electric vehicles (EVs) and portable electronic devices. It is still a great challenge to increase the amount of energy stored in a given system or region of space per unit mass or area or volume.

Among various promising candidates with high energy densities, the lithium-sulfur batteries with a high theoretical capacity of 1675 mAh g^{-1} (3467 mAh cm^{-3}, based on cathode sulfur) and energy density of 2600 Wh kg^{-1} (5382 Wh L^{-1}, based on lithium-sulfur redox couple), respectively, are highly concerned [3-5]. Additionally, elemental sulfur has advantages of low cost, available in abundance both naturally and as industrial by-products, and being environmentally friendly. However, the lithium-sulfur cells still face some challenges: (1) the element sulfur possesses a very low electric conductivity of 5×10^{-30} S cm^{-1} at room temperature, and the poor intrinsic conductivity of sulfur induces the low electrochemical utilization and limited rate capability; (2) there is about 79% volume expansion during the full lithiation of sulfur into Li_2S, which is also insulative; and (3) the dissolved polysulfides in the electrolyte induce a shuttle phenomenon due to their spontaneous redox reaction and freely diffusion in the electrolyte between the anode and cathode, leading to a low capacity and cycling performance. Great efforts have been devoted to enhance the electrical conductivity of the cathodes and suppress the loss of soluble polysulfide intermediates during cycling [6,7]. The conductive scaffolds (*e.g.* ordered mesoporous carbon [8-11], carbon nanotubes (CNTs) [12-15], graphene [16,17], CNT/graphene hybrids [18], carbon hollow spheres [19,20], CNT@micro- [21]/meso-porous carbon [22], carbide-derived carbon [23], hierarchically porous carbon [24], polyaniline [25], *etc.*) are applied to obtain advanced composite cathodes with excellent conductivity, robust electron/ion pathway, as well as superior reversible charge-discharge capacity and cycling performance. The incorporation of porous polysulfide reservoirs [26], polymer chains (such as polyethylene glycol [13,27,28], polyvinylpyrrolidone [29]), Al_2O_3 coating [30], or ion selective membrane [31] affords a chemical gradient that the polysulfides would preferentially be trapped instead of dissolving in the bulk electrolyte.

In most cases, the sulfur loading of C/S composites mostly ranges from 30% to 70% and rarely reaches 80% [8-14,16-21,23,24,32]. The binders, conductive agents, as well as chemical gradient precursors with a ratio of 10-50% were also introduced into the composite cathodes. The introduction of the above-mentioned agents neutralized the advantage of high specified capacity and occupied the effective space. Recently, Ketjen Black, graphene, acetylene black and hollow carbon nanospheres were employed to immobilize 80 wt% sulfur to correlate the carbon properties with the electrochemical behaviors of carbon/sulfur composite cathodes [33]. The graphene-sulfur composites with sulfur fractions of 87 wt% and overall cathode capacity (90 wt% graphene/sulfur + 10 wt% polyvinylidene fluoride binder) of 550 mAh g^{-1} were developed [34]. Porous graphitic carbon with high specific surface area of 1416 m^2 g^{-1} and high pore volume of 1.11 cm^3 g^{-1} was employed to load 88.9 wt% sulfur. The electrode with 70 wt% sulfur/porous graphitic carbon composites, 20 wt% acetylene black and 10 wt% LA132 binder exhibited higher overall discharge capacity of 649.4 mAh $g^{-1}_{(S-C)}$ [35]. Therefore, increasing the energy density of the composite cathodes is still a critical issue to fully demonstrate the advantage of lithium-sulfur cells.

Generally, increasing the sulfur loading in the composite cathode is an efficient and effective way to achieve high energy density. If an interconnect and conductive scaffold with order nanostructures was employed, a large amount of sulfur is expected to be well distributed with a high loading content and improved energy density. Based on this consideration, we explored the idea of embedding sulfur into aligned carbon nanotubes (CNTs) to increase the loading of sulfur up to 90 wt%. The reason why we selected aligned CNTs as the ultra-light conductive scaffolds was that the CNT arrays were with well alignment, hierarchical porous architecture, extremely high conductivity, low density, as well as low cost [36,37]. In addition, the above-mentioned composites avoid the employment of other conductive agents, which is benefitted to improve the practical sulfur loading and energy density. Compared with the super-long aligned CNTs on silicon wafer, the short aligned CNTs grown in fluidized bed were with a very low cost of less than 100 \$ kg^{-1} [38,39]. When the aligned CNTs are distributed into polymer matrix for nanocomposites, aligned CNTs afford an ultralow conductive percolation threshold of 0.0025 wt% [40]. In contrast, the routine agglomerated CNTs have a high conductive percolation threshold of 0.1-4.0 wt% [41]. Therefore, when the aligned CNTs were used as scaffolds to accommodate sulfur, it is expected to build an unblocked conductive network for element sulfur at a very low CNT content. Consequently, the actual loading amount of sulfur can be improved, which provides a facile routine to increase the energy density of lithium-sulfur cells.

Results and discussion

Our concept involves the direct mixing of sulfur and aligned CNTs with a quite high weight ratio for lithium-sulfur cells. As shown in Figure 1a, aligned CNTs with a diameter of 6-12 nm, a length of 20-40 μm, a Brunauer-Emmett-Teller (BET) specific surface area of 208 m^2 g^{-1} were employed as the conductive scaffold to host sulfur. They were grown and packed with homogeneous orientation on the both side of a layered double hydroxide derived flake catalysts. The diameter of aligned CNT bundles was around 1-3 μm (Figure 1a and b). Even after the removal of catalyst flakes, the alignment of CNTs were well preserved, and a pore volume of 0.436 mL g^{-1} was available. During the ball-milling of the aligned CNTs and sulfur powder, the sulfur powders were crushed into small nanoparticles and well distributed into the aligned framework of CNT arrays (Figure 1c). Due to the good alignment and mechanical properties, the CNTs are resilient and can bear the distortion during the ball-milling. Consequently, sulfur particles are tightly trapped by aligned CNTs with well-preserved length. The small bundles of aligned CNTs contact with each other, which renders the as-obtained composites with macroscopic electronic conductivity. The expandable, large volume of the cavity between CNTs provided enough space for sulfur. Therefore, a high sulfur loading of 90 wt% was available while the composite conductivity maintained,

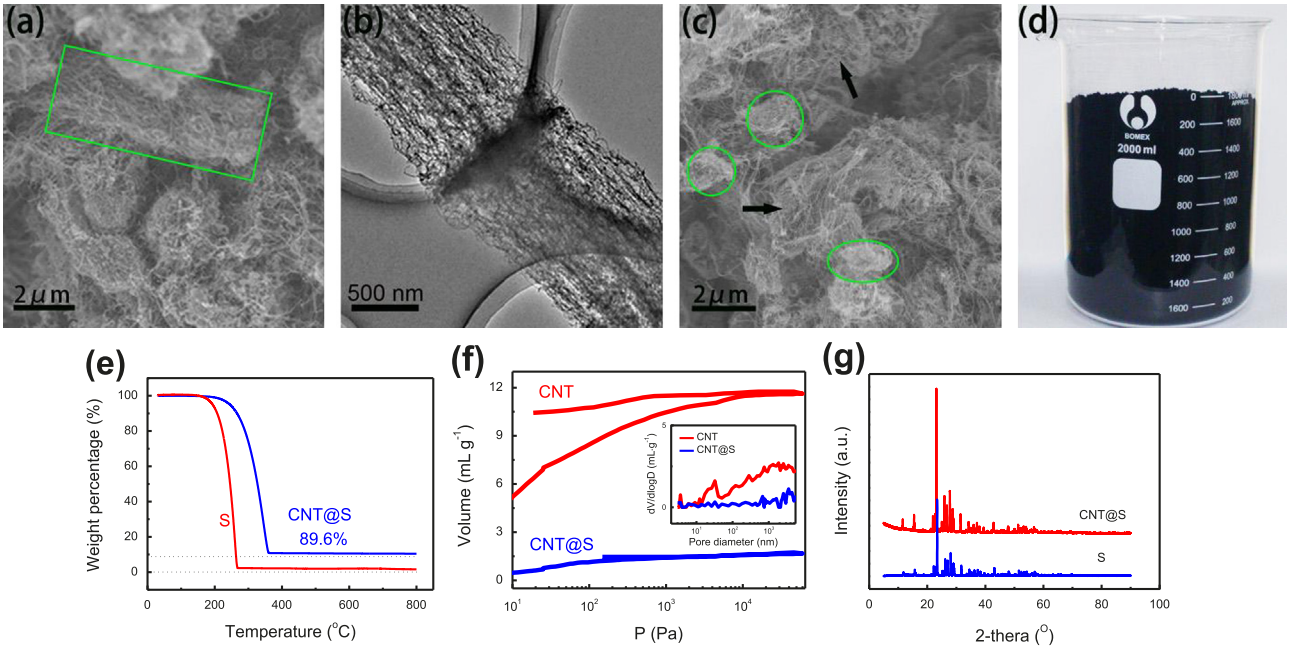

Figure 1 (a) SEM and (b) TEM images of pristine aligned CNTs; (c) SEM image of CNT/sulfur composite cathode, the circles and arrows in (c) refer to the bulk particles of sulfur and aligned CNTs; (d) 2 L CNT/sulfur composite cathode with a sulfur loading of 90 wt% prepared by a facile ball milling; (e) TGA profiles, (f) mercury intrusion curves, and (g) XRD patterns of sulfur and CNT/sulfur composite cathodes. The inset figure in (f) is the pore size distribution calculated from the mercury intrusion profiles.

which is much higher than other nanocarbons (*e.g.* mesoporous carbon [8-11,32] and carbon hollow spheres [42]) with limited space to accommodate sulfur. Herein, no heat annealing of 155 °C was carried out to guarantee the sulfur to be well preserved in the open porous structures of aligned CNTs. Such room-temperature, one-step ball-milling approach towards to high-loading carbon/sulfur composite at kilogram-scale is simple and scalable (Figure 1d), which is of great importance for mass production of composite cathode at a low cost. The amount of sulfur in the composite cathode was determined as 90 wt% by thermogravimetric analysis (TGA) in N_2 atmosphere. The weight loss peak of sulfur in CNT/sulfur cathode shifted to higher temperature range of 260–400 °C (Figure 1e) than that of element sulfur at a temperature range of 200–260 °C, which indicated the strong interactions between the aligned CNT scaffolds and the sulfur. Most of the macro-/meso-pores of the aligned CNT scaffolds were filled by the sulfur (Figure 1f). The pores with a size of 4 and 30 nm disappeared, and those with a size of 50–100 nm significantly decreased after the loading of sulfur. The pore volume decreased from 0.436 to 0.064 mL g^{-1} after loading 90 wt% sulfur. The BET specific surface area of the composite cathode was only 9.41 $m^2 g^{-1}$. The sharp decrease in specific area and pore volume was also confirmed by the SEM image shown as Figure 1c. Therefore, the hierarchically mesopores of aligned CNTs were mostly occupied by the active sulfur for lithium ion storage. The X-ray diffraction (XRD) patterns confirmed the orthorhombic phase of sulfur in composite cathode (Figure 1g).

In order to comprehensively investigate the lithium ion storage performance of the high-sulfur-loading composite cathode, the composite cathode with 90% sulfur was assembled into 2025 type cells with lithium foil as the anode electrode (Figure 2). The properties of cathode materials were listed in Table 1. Although a co-axial CNT@S cable structure is not available yet, the initial mixing status of the cathode does not affect the cycling performance of lithium-sulfur cells, which is similar to the recent reports by Zhang [17]. The discharge capacities were illustrated as Figure 2a. The initial specific discharge capacities calculated by sulfur at a current rate of 0.1C (1C=1672 mA g^{-1}=2.01 mA cm^{-2}) achieved a discharge capacity of 736.8 mAh g^{-1} and 0.893 mAh cm^{-2} based on mass and area of sulfur/carbon composite in the cathode, respectively. A decay rate of 0.96% per cycle was observed at initial 40 cycles. After electrochemical stabilization, a decay rate of 0.23% per cycle and an areal discharge capacity of 0.495 mAh cm^{-2} at 85th cycle were achieved. The 90 wt% CNT/sulfur composite based electrode offered discharge capacities of 789.3, 611.0, 575.4, 475.1, and 140.8 mAh g^{-1} at current rates of 0.05, 0.1, 0.2, 0.5, and 1C, respectively (Figure 2b). The discharge capacity of the lithium-sulfur cells recovered when the current was changed back to 0.05 and/or 0.1C. The poor discharging capacity at 1C was attributed from the slow ion transfer in the electrode induced by the high volume occupation of the active materials in the aligned CNT scaffolds. During each cycle, a two-step discharging behavior was observed, in which two typical plateaus at 2.1–2.25 and 1.9–1.95 V were assigned to the reduction of sulfur to polysulfides and to Li_2S_2 and/or Li_2S, respectively (Figure 2c). During the cycling, the voltage of lower plateaus became lower with 1.95 V in 2nd and 1.9 V in 17th cycle, which was owing to polarization induced by the dissolve of polysulfide into the electrolyte that caused high viscosity electrolyte and blocked the rapid transfer of ions. The accumulating irreversible deposition of Li_2S_2 and/or Li_2S on both cathode

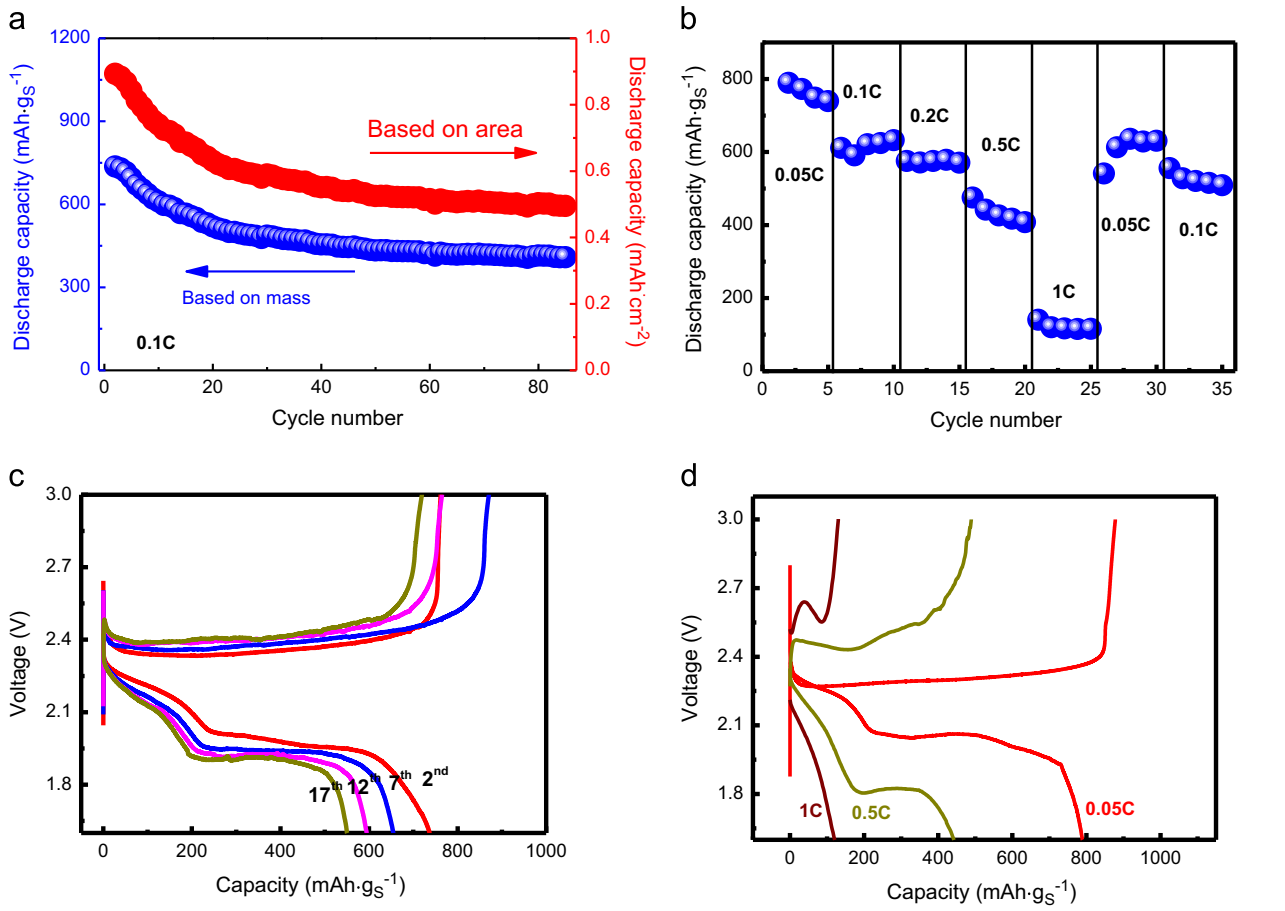

Figure 2 (a) The cycling performance at a current density of 0.1C (1C = 1672 mAh g^{-1}) and (b) the rate performance of CNT/sulfur cathode with sulfur loading of 90 wt%; (c) and (d) were the corresponding Galvanostatic charge-discharge profiles at different cycles and rates, respectively. The capacity is calculated based on sulfur in the cathode.

Table 1 A summary of physical properties and discharge capacities of CNT/sulfur cathode materials with different sulfur loadings.

Sample ID	CNT:S (wt:wt)	Density (mg cm^{-2})	Capacity at 0.1C				
			Density (g cm^{-3})	(mAh g$_S^{-1}$)	(mAh g$_e^{-1}$)	(mAh cm^{-2})	(mAh cm^{-3})
90%	1:9	1.21	1.98	736.8	563.7	0.893	1116.0
80%	2:8	1.01	1.64	742.6	505.4	0.737	818.2
70%	3:7	0.97	1.63	783.2	466.7	0.754	755.4
54%	46:54	0.27	0.40	1097.5	500.3	0.298	200.1

and anode also contributed to the polarization, as well as the loss of the discharge capacity. With the rise of current density, a strong polarization was observed (Figure 2d). This was induced by the effective occupation of micropores and mesopores of the conductive frameworks at high loading of sulfur, which provided very limited ion channels for rapid transfer at large current. It is expected that the rate performance can be greatly improved if a three dimensional porous current collector can be employed [43-45].

When the carbon/sulfur composite was used for a lithium-sulfur cell, the binder, membrane, and anode are included. Therefore, the mass and areal discharge capacity based on the electrode contains the carbon/sulfur composite and binders, as well as volumetric energy density based on volume of cathode, anode, membrane, and the metal current collector were critical values for the practical applications of lithium-sulfur cells. The discharge capacity of the electrode highly depended on the sulfur loading. The controlled cathodes with different sulfur loadings of 54, 70, and 80 wt% (shown in Table 1) were evaluated. The initial discharge capacities of 54, 70, 80, and 90 wt% sulfur loading cathodes were 500.3, 466.7, 505.4, and 563.7 mAh g^{-1} based on the total mass of CNTs/sulfur composites and binders at a current

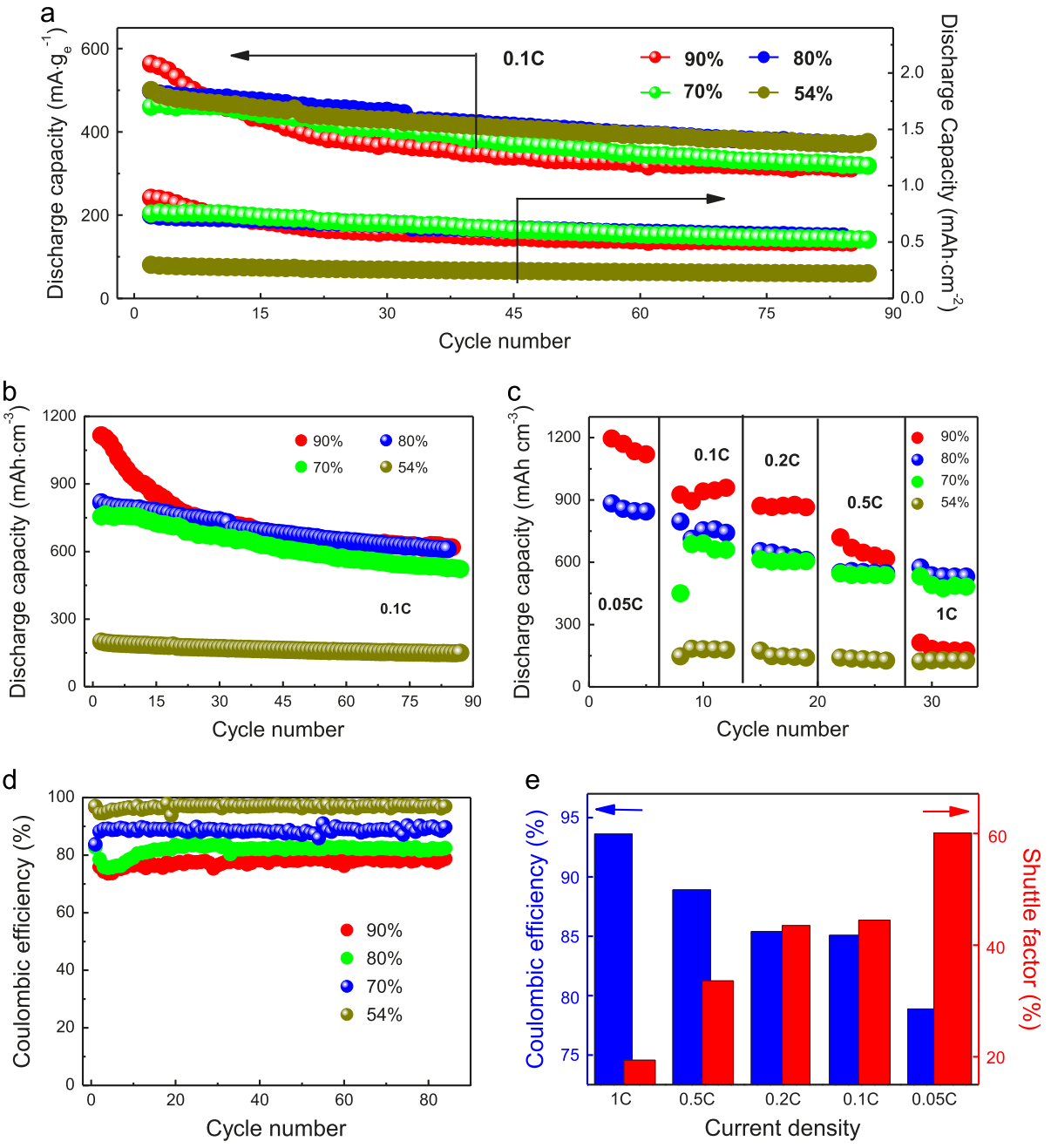

Figure 3 (a) The cycling performance and (b) the rate performance with different sulfur loadings; (c) the Coulombic efficiency of CNT/sulfur cathodes; and (d) the Coulombic efficiency and shuttle factor of sulfur cathode with 90% loading. The discharge capacity herein is calculated based on the total composite cathode included sulfur, carbon, and binders. The volumes of cathode, anode, membrane, as well as the metal current collector were considered for the volumetric discharge capacity.

rate of 0.1C, respectively, corresponding to 0.298, 0.754, 0.737, and 0.893 mAh cm^{-2} (Figure 3a). The high-content of sulfur with 90 wt% loading favors the electrodes with a quite high discharge capacity. Interesting, the tap density of the electrode is sharply increased from 0.40 to 1.98 g cm^{-3} (Table 1) with the rise of sulfur loading from 54 to 90 wt%. Therefore, the volumetric discharge capacity increased from 200.1 to 1116.0 mAh cm^{-3}, which is an improvement by a factor of 5.58 (Figure 3b). However, a competitive volumetric discharge capacity of 738.0 mAh cm^{-3} was available after 30 cycles for 80/90 wt% sulfur loading composites. The reason is inferred to be the rapid irreversible loss of sulfur during charge-discharge process. However, this is still much larger than the discharge capacity of 171.5 mAh cm^{-3} of 54% sulfur loading. The rate performance calculated based on the total composite cathode of sulfur loading of 90, 80, 70 and 54 wt% were shown in Figure 3c. The 90 wt% loading CNT/sulfur composites afforded improved discharge capacities than the lower sulfur loading at every current density. The 70 and 80 wt% loading CNT/sulfur composites exhibited higher capacities than 90% wt% composites at a high current of 1C, indicating the interconnected pores were well preserved in the 70 and 80 wt% loading samples. The aligned CNTs served as

efficient conductive framework to accommodate sulfur, which rendered the rapid ion transfer at high current rates.

The Coulombic efficiency of CNT/sulfur cathodes is also dependent on the loading amount of sulfur. With the increasing sulfur loading amount, more polysulfides were derived from the reduction of sulfur at the cathodes, and they preferred to diffuse to the Li anode, which induced a low Coulombic efficiency and sharp shuttle of polysulfides (Figure 3d). With the rise of the current rate, high Coulombic efficiency was available (Figure 3e). The shuttle factor proposed by Mikhaylik and Akridge [46] was used to reflect the extent of shuttle effect. The value of the shuttle factor in the whole cell increased with the reduction of the current density, indicating the thermodynamically spontaneous diffusion of polysulfides from cathode to anode became gradually dominant.

The energy density and power density were calculated based on the mass of the CNT/sulfur composite. The Ragone plot is shown as Figure 4. The 90 wt% offer an energy densities of 1249.2, 999.9, 900.4, and 686.2 Wh kg^{-1} at a power densities of 134.3, 265.2, 523.5, and 1203.8 W kg^{-1}, respectively. The high loading of sulfur in the composite affords an improved energy density. If the volume of cathode, membrane, anode, and current collector were included, the volumetric energy densities of the CNT/sulfur based cells were calculated. It was plotted with other energy storage devices (a 500 mAh lithium battery, a 25 mF supercapacitor and an electrolytic capacitor of the same absolute capacitance [47]) as Figure 4b. The lithium-sulfur cell with high sulfur loading offered an outstanding rise in their volumetric energy density compared with capacitor and Li ion battery device due to the intrinsic high Li ion storage performance of sulfur. The high sulfur loading amount benefits the dense electrode with high discharge capacity, therefore, the 90 wt% CNT/sulfur composite holds a large increase for the volumetric energy density compared with other routine carbon/sulfur cathode with a low sulfur loading of less than 60 wt%. Compared with other nanostructured carbon with macro-/meso-/micropores, the oriented aligned CNTs with controllable components and sites render high surface area, tunable ordered pore channels, good alignment of building blocks to optimize the electron and ion transport [48]. The open, ordered, straight pores of aligned CNTs facilitate the uniform distribution of fine sulfur particles. The robust sp^2 carbon frameworks are served as rapid pathways for electron transfer. Consequently, aligned CNTs are served as continuous electron highways in the composite cathode. The large aspect ratio, good alignment, ordered packing of each CNT in small bundles offer a low conductive percolation threshold. Even with a very low nanocarbon loading, the sulfur can be efficiently utilized as cathode materials for a lithium-sulfur cell with high volumetric energy density.

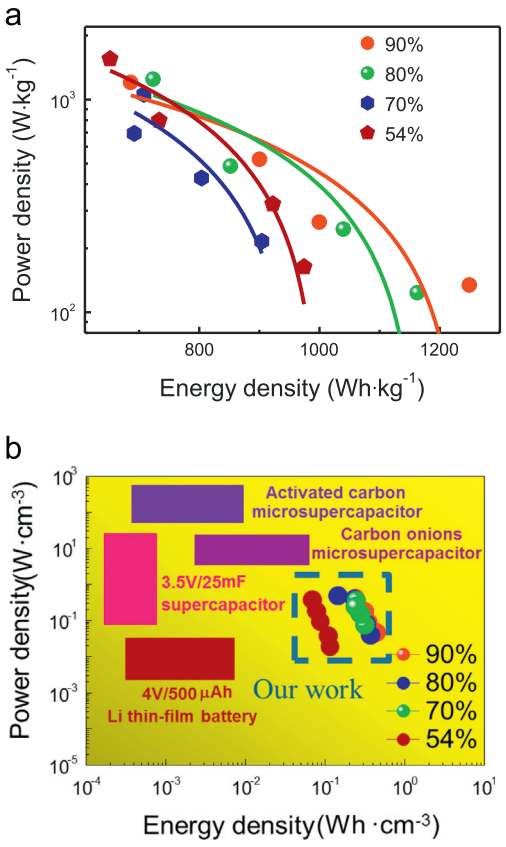

Figure 4 The Ragone plot of CNT/sulfur cathodes with different sulfur loadings. The energy and power density shown in (a) and (b) were calculated by the total composites cathode and the volume of a cell (including cathode, current collector, membrane, and the anode), respectively. The energy density data of supercapacitors and Li ion batteries were collected from Ref. [47].

Conclusions

A composite with high sulfur loading of 90 wt% and a tap density of 1.98 g cm^{-3} was fabricated with aligned CNTs as conductive scaffold by a facile one-step, room temperature ball milling strategy. The mass, areal, volumetric capacities of 90 wt% CNT/sulfur based electrode were 563.7 mAh g^{-1}, 0.893 mAh cm^{-2}, and 1116.0 mAh cm^{-3} based on the whole electrode materials, respectively. Compared with 54 wt% CNT/sulfur composite with a tap density of 0.4 g cm^{-3} and mass/areal/volumetric capacities of 500.3 mAh g^{-1}/0.298 mAh cm^{-2}/200.1 mAh cm^{-3}, there is an outstanding increase in the energy density, which is quite promising for lithium-sulfur cells towards high energy density devices. The use of aligned CNTs to support high loading of sulfur provides not only fundamentally new insight into the transport of electrons and ions in complex nanostructures, but also the facile strategy to improve the lithium storage performance. Further effort into composite fabrication and system optimization to fully demonstrate the potentials of ordered nanostructures for lithium-sulfur batteries with superior energy density and rate performance is still required.

Experimental

Composite cathode fabrication

The aligned CNTs were mass-produced on a FeMgAl layered double hydroxide derived flake catalysts [49] in a fluidized bed reactor. The as-grown carbon products were purified by NaOH (12.0 mol L^{-1}) aqueous solution at 160 °C for 4 h and

HCl (5.0 mol L^{-1}) aqueous solution at 70 °C for 4 h, subsequently, which is similar to our previous publication [50]. The high purity aligned CNT bundles were available after filtering, washing, and freeze-drying. Then the CNTs were mixed with sulfur powder in the anticipated ratio and ball-milled for 3 h to form CNT/sulfur cathode.

Structure characterizations

A JSM 7401F SEM (JEOL Ltd., Tokyo, Japan) at 1.0 kV and a TEM (JEOL Ltd., Tokyo, Japan) at 120.0 kV were employed to detect the morphology of cathodes. The Raman spectra of the CNT and CNT/sulfur cathode were recorded using Horiba Jobin Yvon LabRAM HR800 Raman spectrometer (He-Ne laser excitation at 633 nm). The sulfur content of CNT/sulfur composite was determined by TGA using TGA/DSC1 STAR^e system with N_2 atmosphere and a temperature ramp rate of 10 °C min^{-1}. The N_2 adsorption-desorption isotherms were collected by using an N_2 adsorption analyzer (Autosorb-IQ_2-MP-C system) at 77 K. The sample was degassed at a low temperature of 50 °C until a manifold pressure of 2 mm Hg was reached before N_2 sorption isotherm measurements to avoid the sulfur sublimation. The surface area was determined by the BET method. The distribution plot of extensive pore size was determined by an *ex situ* Hg penetration method. The structure of the cathode was identified by an XRD (D8-Advance, Bruker, Germany). The tap density of samples was determined by calculating the ratio of the mass of the measured material to its tapped volume.

Li storage performance on composite cathode

The CNT/sulfur composite cathode was fabricated with poly (vinylidene fluoride) (PVDF) binder in N-methyl-2-pyrrolidone (NMP) with a mass ratio of CNT/sulfur: PVDF=85:15. A homogeneously mixed slurry was prepared by magnetic stirred for *ca.* 24 h. The slurry was then coated onto a 25-μm-thick Al foil by a doctor blade. The obtained electrode was dried in a vacuum drying oven at 60 °C for 12.0 h. After that, the foil was punched into 13 mm disks as the working cathodes. The electrodes were assembled in a two-electrode cells configuration using standard 2025 coin-type cells. One millimeter thick Li metal foil was selected as a counter electrode. The mixed solution of 1,3-dioxolane (DOL) and 1,2-dimethoxyethane(DME) (v/v=1/1) with 1 mol L^{-1} lithium bis(trifluoromethanesulfonyl)imide (LiTFSI) as the electrolyte, and the Celgard 2400 polypropylene membranes as the separator. The assembling of cells was conducted in an Ar-filled glove box with oxygen and water content below 1 ppm. The coin cells were monitored in galvanostatic mode within a voltage range of 1.6–3.0 V using Neware multichannel battery cycler. A typical cell contained a cathode loading of approximately 1.6 mg of sulfur.

The Ragone plots were calculated based on experimental discharge capacity and voltage at different currents and sulfur loadings. The energy/power density shown in Figure 4a was calculated based on the mass of carbon/sulfur composites cathode. The energy/power density illustrated in Figure 4b was derived from the volume of total cell, including cathode, current collector, membrane, anode. The anode was estimated by assuming the complete reaction of lithium and sulfur into Li_2S (*e.g.*, the thickness of the cathode, current collector, membrane, anode of 90% sulfur loading cell were 8, 10, 25, 2.56 μm, respectively).

Acknowledgments

This work was supported by the National Natural Science Foundation of China (21306103) and China Postdoctoral Science Foundation (2012M520293, 2013T60125).

References

[1] N.S. Choi, Z.H. Chen, S.A. Freunberger, X.L. Ji, Y.K. Sun, K. Amine, G. Yushin, L.F. Nazar, J. Cho, P.G. Bruce, Angew. Chem. Int. Ed. 51 (2012) 9994.
[2] J.T. Xu, S.X. Dou, H.K. Liu, L.M. Dai, Nano Energy 2 (2013) 439.
[3] P.G. Bruce, S.A. Freunberger, L.J. Hardwick, J.M. Tarascon, Nat. Mater. 11 (2012) 19.
[4] M.K. Song, E.J. Cairns, Y.G. Zhang, Nanoscale 5 (2013) 2186.
[5] S.S. Zhang, J. Power Sour. 231 (2013) 153.
[6] D.W. Wang, Q.C. Zeng, G.M. Zhou, L.C. Yin, F. Li, H.M. Cheng, I.R. Gentle, G.Q.M. Lu, J. Mater. Chem. A 1 (2013) 9382.
[7] Y. Yang, G.Y. Zheng, Y. Cui, Chem. Soc. Rev. 42 (2013) 3018.
[8] X. Ji, K.T. Lee, L.F. Nazar, Nat. Mater. 8 (2009) 500.
[9] F.G. Sun, J.T. Wang, H.C. Chen, W.C. Li, W.M. Qiao, D.H. Long, L.C. Ling, ACS Appl. Mater. Interfaces 5 (2013) 5630.
[10] D. Li, F. Han, S. Wang, F. Cheng, Q. Sun, W.C. Li, ACS Appl. Mater. Interfaces 5 (2013) 2208.
[11] M. Oschatz, S. Thieme, L. Borchardt, M.R. Lohe, T. Biemelt, J. Bruckner, H. Althues, S. Kaskel, Chem. Commun. 49 (2013) 5832.
[12] G.M. Zhou, D.W. Wang, F. Li, P.X. Hou, L.C. Yin, C. Liu, G.Q. Lu, I.R. Gentle, H.M. Cheng, Energy Environ. Sci. 5 (2012) 8901.
[13] S.M. Zhang, Q. Zhang, J.Q. Huang, X.F. Liu, W.C. Zhu, M.Q. Zhao, W.Z. Qian, F. Wei, Part. Part. Syst. Charact. 30 (2013) 158.
[14] M. Hagen, S. Dorfler, H. Althues, J. Tubke, M.J. Hoffmann, S. Kaskel, K. Pinkwart, J. Power Sour. 213 (2012) 239.
[15] M. Hagen, S. Dorfler, P. Fanz, T. Berger, R. Speck, J. Tubke, H. Althues, M.J. Hoffmann, C. Scherr, S. Kaskel, J. Power Sour. 224 (2013) 260.
[16] G. Zhou, L.-C. Yin, D.-W. Wang, L. Li, S. Pei, I.R. Gentle, F. Li, H.-M. Cheng, ACS Nano 7 (2013) 5367.
[17] J.Q. Huang, X.F. Liu, Q. Zhang, C.M. Chen, M.Q. Zhao, S.M. Zhang, W.C. Zhu, W.Z. Qian, F. Wei, Nano Energy 2 (2013) 314.
[18] M.Q. Zhao, X.F. Liu, Q. Zhang, G.L. Tian, J.Q. Huang, W.C. Zhu, F. Wei, ACS Nano 6 (2012) 10759.
[19] N. Brun, K. Sakaushi, L.H. Yu, L. Giebeler, J. Eckert, M.M. Titirici, Phys. Chem. Chem. Phys. 15 (2013) 6080.
[20] C.F. Zhang, H.B. Wu, C.Z. Yuan, Z.P. Guo, X.W. Lou, Angew. Chem. Int. Ed. 51 (2012) 9592.
[21] S. Xin, L. Gu, N.H. Zhao, Y.X. Yin, L.J. Zhou, Y.G. Guo, L.J. Wan, J. Am. Chem. Soc. 134 (2012) 18510.
[22] R. Xu, I. Belharouak, J.C.M. Li, X. Zhang, I. Bloom, J. Bareño, Adv. Energy Mater. 3 (2013) 833.
[23] J.T. Lee, Y. Zhao, S. Thieme, H. Kim, M. Oschatz, L. Borchardt, A. Magasinski, W.I. Cho, S. Kaskel, G. Yushin, Adv. Mater. 25 (2013) 4573.
[24] L. Yu, N. Brun, K. Sakaushi, J. Eckert, M.M. Titirici, Carbon 61 (2013) 245.
[25] J.L. Wang, J. Yang, J.Y. Xie, N.X. Xu, Adv. Mater. 14 (2002) 963.
[26] X.L. Ji, S. Evers, R. Black, L.F. Nazar, Nat. Commun. 2 (2011) 325.

[27] H. Wang, Y. Yang, Y. Liang, J.T. Robinson, Y. Li, A. Jackson, Y. Cui, H. Dai, Nano Lett. 11 (2011) 2644.
[28] X.L. Ji, K.T. Lee, L.F. Nazar, Nat Mater. 8 (2009) 500.
[29] G.Y. Zheng, Q.F. Zhang, J.J. Cha, Y. Yang, W.Y. Li, Z.W. Seh, Y. Cui, Nano Lett. 13 (2013) 1265.
[30] X. Han, Y. Xu, X. Chen, Y.-C. Chen, N. Weadock, J. Wan, H. Zhu, Y. Liu, H. Li, G. Rubloff, C. Wang, L.B. Hu, Nano Energy 2 (2013) 1197.
[31] J.-Q. Huang, Q. Zhang, H.-J. Peng, X.-Y. Liu, W.-Z. Qian, F. Wei, Energy Environ. Sci. 7 (2014) 353.
[32] D.W. Wang, G.M. Zhou, F. Li, K.H. Wu, G.Q. Lu, H.M. Cheng, I.R. Gentle, Phys. Chem. Chem. Phys. 14 (2012) 8703.
[33] J.M. Zheng, M. Gu, M.J. Wagnerb, K.A. Hays, X.H. Li, P.J. Zuo, C.M. Wang, J.G. Zhang, J. Liu, J. Xiao, J. Electrochem. Soc. 160 (2013) A1624.
[34] S. Evers, L.F. Nazar, Chem. Commun. 48 (2012) 1233.
[35] G.-L. Xu, Y.-F. Xu, J.-C. Fang, X.-X. Peng, F. Fu, L. Huang, J.-T. Li, S.-G. Sun, ACS Appl. Mater. Interfaces 5 (2013) 10782.
[36] C.M. Seah, S.P. Chai, A.R. Mohamed, Carbon 49 (2011) 4613.
[37] Q. Zhang, J.-Q. Huang, W.-Z. Qian, Y.-Y. Zhang, F. Wei, Small 9 (2013) 1237.
[38] Q. Zhang, M.Q. Zhao, J.Q. Huang, Y. Liu, Y. Wang, W.Z. Qian, F. Wei, Carbon 47 (2009) 2600.
[39] Q. Zhang, J.-Q. Huang, M.-Q. Zhao, W.-Z. Qian, F. Wei, ChemSusChem 4 (2011) 864.
[40] J.K.W. Sandler, J.E. Kirk, I.A. Kinloch, M.S.P. Shaffer, A.H. Windle, Polymer 44 (2003) 5893.
[41] W. Bauhofer, J.Z. Kovacs, Compos. Sci. Technol. 69 (2009) 1486.
[42] F. Bottger-Hiller, P. Kempe, G. Cox, A. Panchenko, N. Janssen, A. Petzold, T. Thurn-Albrecht, L. Borchardt, M. Rose, S. Kaskel, C. Georgi, H. Lang, S. Spange, Angew. Chem. Int. Ed. 52 (2013) 6088.
[43] L.C. Yin, J.L. Wang, F.J. Lin, J. Yang, Y. Nuli, Energy Environ. Sci. 5 (2012) 6966.
[44] H. Kim, J.T. Lee, G. Yushin, J. Power Sour. 226 (2013) 256.
[45] J. Jin, Z.Y. Wen, G.Q. Ma, Y. Lu, Y.M. Cui, M.F. Wu, X. Liang, X.W. Wu, RSC Adv. 3 (2013) 2558.
[46] Y.V. Mikhaylik, J.R. Akridge, J. Electrochem. Soc. 151 (2004) A1969.
[47] D. Pech, M. Brunet, H. Durou, P.H. Huang, V. Mochalin, Y. Gogotsi, P.L. Taberna, P. Simon, Nat. Nanotechnol. 5 (2010) 651.
[48] J.Q. Huang, Q. Zhang, S.M. Zhang, X.F. Liu, W.C. Zhu, W.Z. Qian, F. Wei, Carbon 58 (2013) 99.
[49] Q. Zhang, M.-Q. Zhao, D.-M. Tang, F. Li, J.-Q. Huang, B. Liu, W.-C. Zhu, Y.-H. Zhang, F. Wei, Angew. Chem. Int. Ed. 49 (2010) 3642.
[50] T.-C. Chen, M.-Q. Zhao, Q. Zhang, G.-L. Tian, J.-Q. Huang, F. Wei, Adv. Functional Mater. 23 (2013) 5066.

Xin-Bing Cheng obtained his bachelor's Degree in Chemical Engineer, Tianjin University, China in 2012. Now, he is a graduate student in Tsinghua University, China. His research interests are the fundamental energy science and commercial application of carbon nanotube, graphene, and lithium-sulfur battery.

Jia-Qi Huang received his Ph.D degree from department of chemical engineering, Tsinghua University, China. He was a visiting researcher in Prof. P.M. Ajayan's group at Rice University, USA in 2010. His research interests are the mass production of CNTs/graphene as well as their applications in energy conversion and storage, especially for Li-S batteries and Li ion batteries.

Qiang Zhang graduated in 2004 from the department of chemical engineering, Tsinghua University, China, where he continued doing research on mass production of carbon nanotubes and obtained his Ph.D in chemical engineering in 2009. After a short stay as a research associate in Case Western Reserve University, USA in 2009, he joined the Fritz Haber Institute of the Max Planck Society, Germany as a post-doctoral fellow. He was appointed an associate professor of chemical engineering of Tsinghua University in 2011. His current research interests are nanocarbon, advanced functional materials, sustainable chemical engineering, energy conversion and storage.

Hong-Jie Peng gained his Bachelor's degree from Department of Chemical Engineering, Tsinghua University, P.R. China and is currently a Ph. D. candidate at Tsinghua University. His research interests focus on nanocarbon, advanced functional materials, high-performance lithium batteries, and novel energy storage devices.

Meng-Qiang received his Ph.D degree from department of chemical engineering, Tsinghua University, China. He had been a one year visiting scholar at University of Virginia, USA. His research interests are synthesis chemistry, mass production, assembly, electrochemical energy storage of CNTs and lamellar particles.

Fei Wei obtained his Ph.D in chemical engineering from China University of Petroleum in 1990. After a postdoctoral fellowship at Tsinghua University, he was appointed as an associate professor in 1992 and professor of chemical engineering of Tsinghua University in 1996. He was also a Visiting Professor at Ohio State University (USA), University of Western Ontario (Canada), and Nagoya Institute of Science and Technology (Japan). Now he is the director of the Fluidization Laboratory of Tsinghua University. His scientific interests are chemical reaction engineering, multiphase flow, advanced materials, and sustainable energy.